ELSEVIER

Catalysis Today 38 (1997) 3–12

CATALYSIS TODAY

On the dynamic behavior of automotive catalysts

T. Kirchner*, G. Eigenberger

Institut für Chemische Verfahrenstechnik, Universität Stuttgart, Böblingerstr. 72, D-70199 Stuttgart, Germany

Abstract

Automotive catalytic converters show highly transient operation due to fluctuating exhaust gas conditions in real application. Local ignition of the reactions with very steep temperature gradients as well as moving reaction fronts can occur in the monolithic catalyst. Theoretical investigations are presented based upon detailed simulation studies with a one-dimensional two-phase model for the catalytic converter. The simulation of the heat-up of the automotive catalyst during the cold-start shows a highly transient behavior for different cold-start concepts. Also, hot spot phenomena can be observed in the simulation under specific exhaust gas conditions.

Keywords: Automotive converter; Catalytic combustion; Monolithic reactor; Dynamic behavior; Numerical simulation

1. Introduction

Three-way catalysts (TWC) that control the vehicle emissions of hydrocarbons (HCs), carbon monoxide (CO) and nitrogen oxides (NO_x) are an effective way to reduce automotive exhaust emissions. Automotive catalytic converters represent an example of fixed bed reactors under highly transient operating conditions due to strongly fluctuating inlet conditions, namely exhaust gas temperature, mass flow and gas composition (Fig. 1) [1]. Under these conditions, local ignition of the reactions resulting in so-called hot spots at the catalytic surface as well as moving reaction fronts can occur in the monolithic catalyst. The occurrence of extreme local temperature peaks at the catalytic surface is well known in the operation of automotive catalysts. They are considered to have a considerable influence on the catalyst aging [2].

In spite of these unfavorable working conditions the automotive catalyst reaches a conversion efficiency of more than 95%. A minimum temperature of approximately 350°C at the catalyst is required for proper combustion. The necessary heat for start-up is provided, e.g., by the hot exhaust gas stream. Due to the heat capacity of the exhaust system it takes about 1–2 min after the start of the engine before this temperature level is reached. The main source of pollutants is during this period. Presently the main approaches to lower the emissions during cold-start are the use of an electrically heated pre-catalyst (EHC) [3–6] and a burner-heated catalyst (BHC) [7–9]. The EHC uses the electrical power supplied by the car battery to heat the catalyst. In the case of BHC, gasoline is burned to obtain a hot exhaust gas stream which heats the main catalyst faster. Using these cold-start concepts the behavior of the catalytic converter is characterized by highly transient operating conditions because of the rapid warm-up of the catalyst and the

*Corresponding author. Tel.: (49-214) 305-6687.

PII S0920-5861(97)00033-3

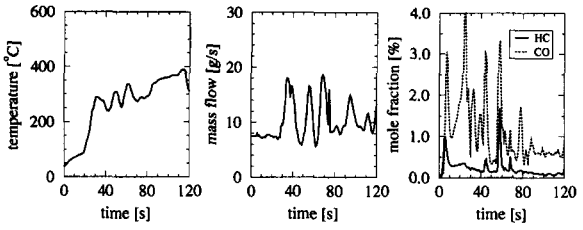

Fig. 1. Inlet conditions of the automotive catalyst during part of the FTP-75 test cycle for a specific SI-engine (4 cylinders, 2.0 l).

resulting ignition of the catalytic reactions at the converter.

This contribution reports on a joint research project with Volkswagen AG to investigate the dynamic behavior of automotive catalytic converter systems with an emphasis on the behavior during start-up. Possible sources for the occurrence of hot spots are also determined and the influence of important parameters is discussed. Detailed simulation studies are used to describe the transient thermal and conversion characteristics of the TWC.

2. Mathematical model

The mathematical model for the catalytic converter used here is one-dimensional and incorporates separate energy and mass balances for gas and solid phases.

- Energy balance for the gas phase (gas temperature υ_g)

$$\epsilon \cdot \rho_g \cdot c_{p,g} \cdot \frac{\partial \upsilon_g}{\partial t} = -G_z \cdot c_{p,g} \cdot \frac{\partial \upsilon_g}{\partial z} + \epsilon \cdot \lambda_{\text{eff}} \cdot \frac{\partial^2 \upsilon_g}{\partial z^2} + \alpha_{s,g}(z) \cdot a_v \cdot (\upsilon_s - \upsilon_g). \quad (1)$$

- Energy balance of the solid phase (solid temperature υ_s)

$$(1-\epsilon) \cdot \rho_s \cdot c_{p,s} \cdot \frac{\partial \upsilon_s}{\partial t} = (1-\epsilon) \cdot \lambda_s \cdot \frac{\partial^2 \upsilon_s}{\partial z^2} + a_x \cdot \sum_{i=1}^{I} (-\Delta h_{r,i}) \cdot R_i \quad (2)$$
$$- \alpha_{s,g}(z) \cdot a_v \cdot (\upsilon_s - \upsilon_g)$$
$$- \alpha_{s,\text{amb}} \cdot a_{\text{ext}} \cdot (\upsilon_s - \upsilon_{\text{amb}}) + \dot{q}_{\text{el}}.$$

- Mass balance of the gas phase (weight fraction $w_{j,g}$)

$$\epsilon \cdot \rho_g \cdot \frac{\partial w_{j,g}}{\partial t} = -G_z \cdot \frac{\partial w_{j,g}}{\partial z} + \epsilon \cdot D_{\text{eff}} \frac{\partial^2 w_{j,g}}{\partial z^2} - \rho_g \cdot \beta_j(z) \cdot a_v \cdot (w_{j,g} - w_{j,s}). \quad (3)$$

- Mass balance of the solid phase (weight fraction $w_{j,s}$)

$$0 = \rho_g \cdot \beta_j(z) \cdot a_v \cdot (w_{j,g} - w_{j,s}) - a_x \cdot M_j \cdot \sum_{i=1}^{I} \nu_{ij} \cdot R_i. \quad (4)$$

- Danckwerts boundary conditions at the inlet and outlet

$$G_z \cdot c_{p,g} \cdot \upsilon_{G,\text{in}} = G_z \cdot c_{p,g} \cdot \upsilon_g - \epsilon \cdot \lambda_{\text{eff}} \cdot \frac{\partial \upsilon_g}{\partial z}, \quad (5)$$

$$G_z \cdot w_{G,\text{in}} = G_z \cdot w_g - \epsilon \cdot D_{\text{eff}} \cdot \frac{\partial w_g}{\partial z}, \quad (6)$$

$$\left.\frac{\partial \upsilon_s}{\partial z}\right|_{z=0} = 0, \quad (7)$$

$$\left.\frac{\partial \upsilon_g}{\partial z}\right|_{z=L} = \left.\frac{\partial \upsilon_s}{\partial z}\right|_{z=L} = \left.\frac{\partial w_g}{\partial z}\right|_{z=L} = 0. \quad (8)$$

The model considers the most important reactions for the start-up. The combustion of the key components CO, propene, propane and hydrogen is described by kinetic rate expressions according to the following reaction scheme:

$$H_2 + \tfrac{1}{2}O_2 \rightarrow H_2O$$

$$CO + \tfrac{1}{2}O_2 \rightarrow CO_2$$

$$C_3H_6 + \tfrac{9}{2}O_2 \rightarrow 3CO_2 + 3H_2O$$

$$C_3H_6 + 5O_2 \rightarrow 3CO_2 + 4H_2O$$

A more detailed description of the model with the underlying assumptions and the spatially non-uniform heat and mass transfer between exhaust gas and the catalytic surface is given elsewhere [10].

3. Cold-start behavior of different converter systems

The cold-start behavior of the catalytic converter consisting of the main catalyst only (Fig. 2) is

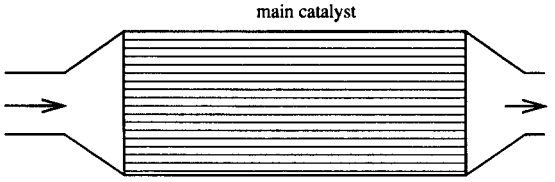

Fig. 2. Automotive converter consisting of the main catalyst only.

described in the following. Fig. 3 shows temperature and concentration profiles of CO, propene and propane at different times of the cold-start test cycle. Because of the time dependent conditions at the inlet of the converter, the concentration profiles are always normalized with respect to the inlet concentrations at each time step. The lower diagrams of Fig. 3 compare the time course of the concentrations of CO and the hydrocarbons (HCs) (propene and propane) in the feed and exit of the catalytic converter.

When the engine is started (t=0 s), both the exhaust pipe and the catalyst are at ambient temperature (υ_{amb}=20°C) and no pollutants are converted at the catalyst. The entrance of the main catalyst is only slowly heated up by the exhaust gas stream and in this specific case no conversion of CO and the HCs takes place until 28 s after the engine was started. Then the heat of reaction set free on the catalytic surface causes a rapid ignition and total combustion of the pollutants is reached after 60 s.

In order to shorten the start-up period an EHC can be used which is located in front of the main catalyst (Fig. 4). The presently used EHC is a two-brick design. It consists of a short metallic monolith which is heated by the car battery and a second, larger but unheated monolith. This second monolith enlarges the catalytic surface area and ensures the mechanical stability of the whole EHC construction. The design of this EHC was obtained by optimization based upon extensive experimental and simulation studies [10,11]. It was shown that future legislative requirements can be fulfilled with this EHC. The cold-start behavior of the catalytic converter system with EHC is shown in Fig. 5. Again the simulation starts with a temperature level of 20°C over the entire length of the exhaust pipe. Five seconds after the start of the engine the heated brick reaches a temperature of approximately 400°C. At this time, the reduction of the HC emission is still low because of the very small catalytic surface of the heated brick. As a result of the good convective heat transport, the second brick of the EHC reaches ignition temperature level fast. Thus the conversion of the pollutants can be increased to 80–90% within 9 s. The electrical heating of the first brick plus the reaction heat set free at the EHC help to warm-up the main catalyst and total combustion of the HCs is completed only after 25 s.

The maximum available electrical power from the car battery is only approximately 1.5 kW. Due to the limitation of available power in the case of the EHC cold-start concept, the use of a burner-heated catalyst (BHC, Fig. 6) was investigated as a possible alternative. By burning the fuel directly the available power is much higher compared to the EHC approach. Experimental studies are published in literature with burners of up to 15 kW [8]. As the fuel is burned under steady-state conditions, the emission of pollutants in the burner exhaust gas should be negligible. Fig. 7 shows the results of a simulation run for a 13 kW burner. Depending on the configuration of burner and catalyst, the inlet temperature of the catalyst is rising up to approximately 800°C within 20 s due to the mixing of the hot burner exhaust with the exhaust gas stream of the engine. This leads to a very fast onset of the conversion of all pollutants at the catalytic converter. Nevertheless, it takes a few seconds to move the temperature front into the monolith in order to widen the reaction zone. For this reason total conversion of the HCs is still limited to approximately 70% after 7 s. Due to the strong power input, total combustion of CO and the hydrocarbon can be reached after 8 and 15 s, respectively. In fact the heat-up of the TWC is slightly faster compared to the EHC concept, but nevertheless the cold-start emissions especially of the HCs are much higher in the case of using the BHC. This is due to the production of additional pollutants by the combustion of gasoline in the external burner. The increase of the HC emissions after the start of the burner can be clearly seem in the lower diagrams of Fig. 7. During the first few seconds the outlet concentrations of the HCs exceed the raw emissions produced by the engine.

There are some more disadvantages using an external burner, which can also be seen from the simulation results. When starting the engine, the entrance of the catalyst is rapidly exposed to very high temperatures. This may affect the long term stability of the catalytic washcoat on the monolith due to thermal shock.

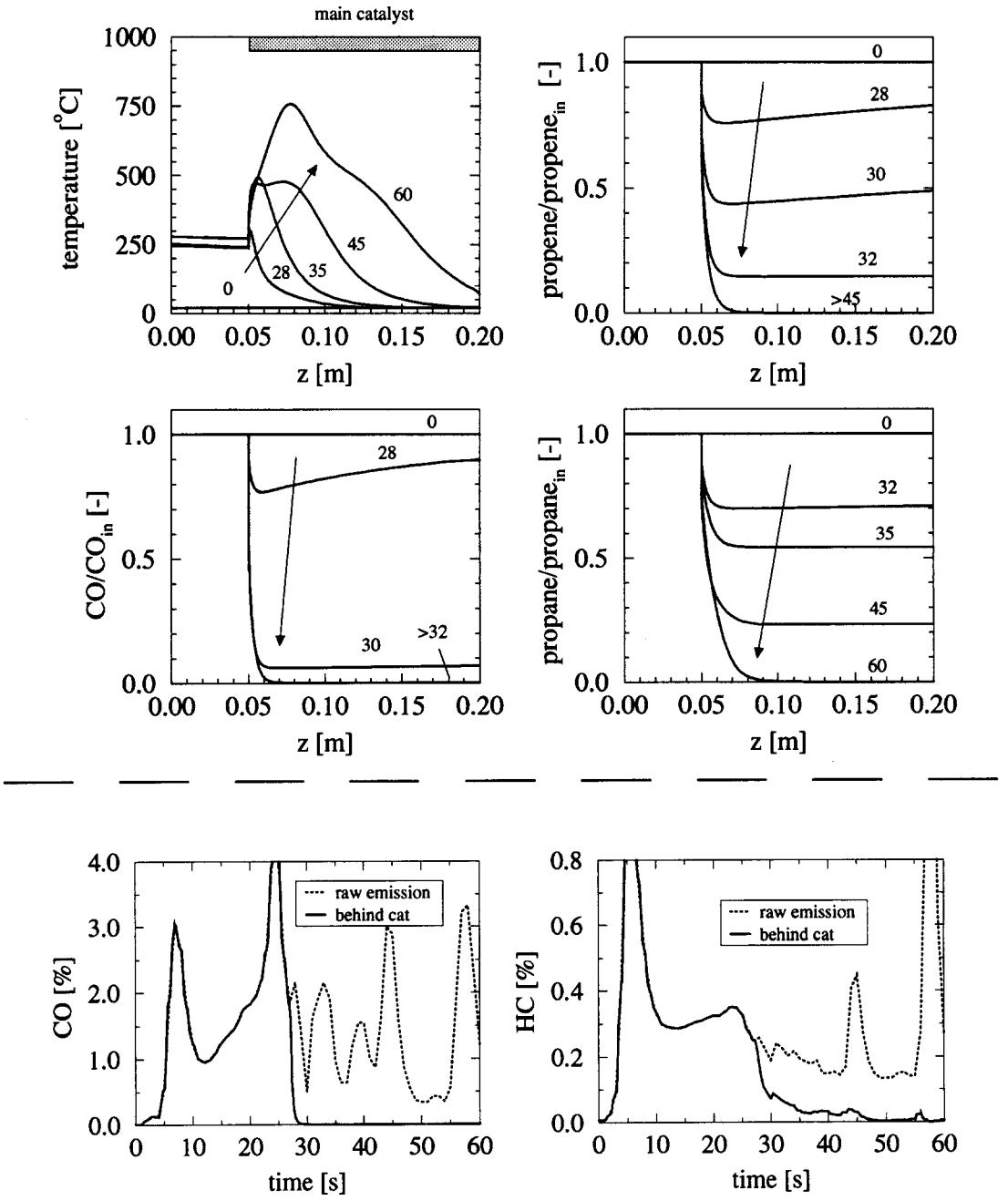

Fig. 3. Cold-start behavior of the main catalyst (all times are given in seconds).

Furthermore, due to the reaction heat set free at the catalytic surface a maximum temperature level of 900°C can be reached at the entrance of the converter. Since the maximum temperature is depending on the amount of burned pollutants it may lead to a faster local deactivation of the catalyst and consequently to a gradual deterioration of the conversion behavior of the catalytic converter during cold-start.

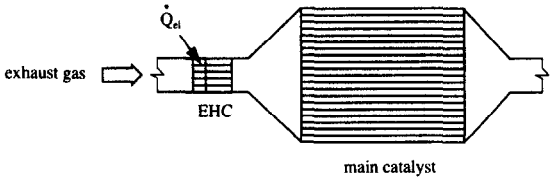

Fig. 4. Electrically heated pre-catalyst (EHC).

These examples show that highly transient operation conditions occur in automotive catalytic converters during cold-start.

4. Hot spot phenomena

The occurrence of extreme local temperature peaks (hot spots) at the catalytic surface is well known in real application of automotive catalysts. These hot spots causes severe deactivation of the catalyst due to local sintering of the washcoat or even melting of the ceramic matrix. Presently in spite of its importance, the reason for this phenomenon is still unknown. It is known that the catalyst must already be at working temperatures to enable high reaction rates and a strong heat release by reaction. Additionally, the concentration of pollutants at the catalytic surface should increase locally to cause a rapid combustion of the pollutants. For this reason, the occurrence of hot spots usually is attributed to HC peaks in the exhaust gas stream.

Due to the complex interactions of the inlet conditions (temperature, mass flow and composition) with the catalyst, one can imagine also other reasons for the occurrence of hot spots. The subsequent simulations were made under the following assumptions:

- The converter system consists only of the main catalyst.
- The simulation always starts at steady state conditions at the catalyst.
- Changes of the inlet conditions are restricted to mass flow and gas temperature. In particular, varying inlet concentrations are excluded.
- The reaction scheme is reduced to the oxidation reactions of CO and H_2. Other components are omitted. The oxidation of CO and H_2 show rapid light-off which might be important for hot-spot occurrence. Due to this simplification, less reaction he at is set free compared to real conditions. In order to compensate (numerically) the neglected combustion of the HCs (0.13% propene and 0.13% propane) the reaction heat of the CO oxidation is increased by a factor of 2.3.

Fig. 8 shows an example for the simulation of the hot spot phenomenon. The simulation starts at the time t_0. At this time it is assumed that the catalyst is already hot and the engine runs idle (exhaust mass flow $\dot{m} = 7$ g/s and gas temperature υ_g=280°C). The diagrams in the first column of Fig. 8 show the temperature and CO concentration profiles versus the length of the catalyst at the resulting steady state. Hydrogen is always burned completely at the first few millimeters of the monolith and does not effect the occurrence of hot-spots in this example. Hence, the concentration profiles of hydrogen are omitted in Fig. 8. Due to the low temperature level only H_2 is burned at the catalyst entrance. This leads to a small temperature rise at the beginning of the monolith. The light-off temperature of the CO oxidation is reached at $z \approx 0.08$ m and CO is completely consumed further down-stream. Due to the reaction heat of the CO oxidation (plus HCs) a certain temperature rise occurs at this location. The monolith can be roughly divided into a colder and a hotter part. The temperature profiles of the gas phase and the solid phase are almost identical because of the low mass flow and the good heat transport from the catalytic surface to the gas phase.

Assuming that the car is accelerated at $t=t_0$, the mass flow increases to $\dot{m} = 50$ g/s within 1 s and also the exhaust gas temperature is rising up to υ_g=400°C. The diagrams in the second column of Fig. 8 show the profiles 1 s after the acceleration took place. As mentioned before, the inlet concentrations of CO and H_2 are kept constant all the time. Due to the increasing mass flow the concentrations profiles and the temperature profile of the gas phase are shifted into the rear of the catalyst. However, the temperature profile of the solid phase is almost unchanged because of the larger heat capacity of the monolith. Since the CO concentration profile is shifted into the hotter part of the catalyst a rapid increase of the CO concentration on the catalytic surface is caused. Due to the high temperatures CO is rapidly burned at the beginning of the hotter part of the monolith. This leads to a transient

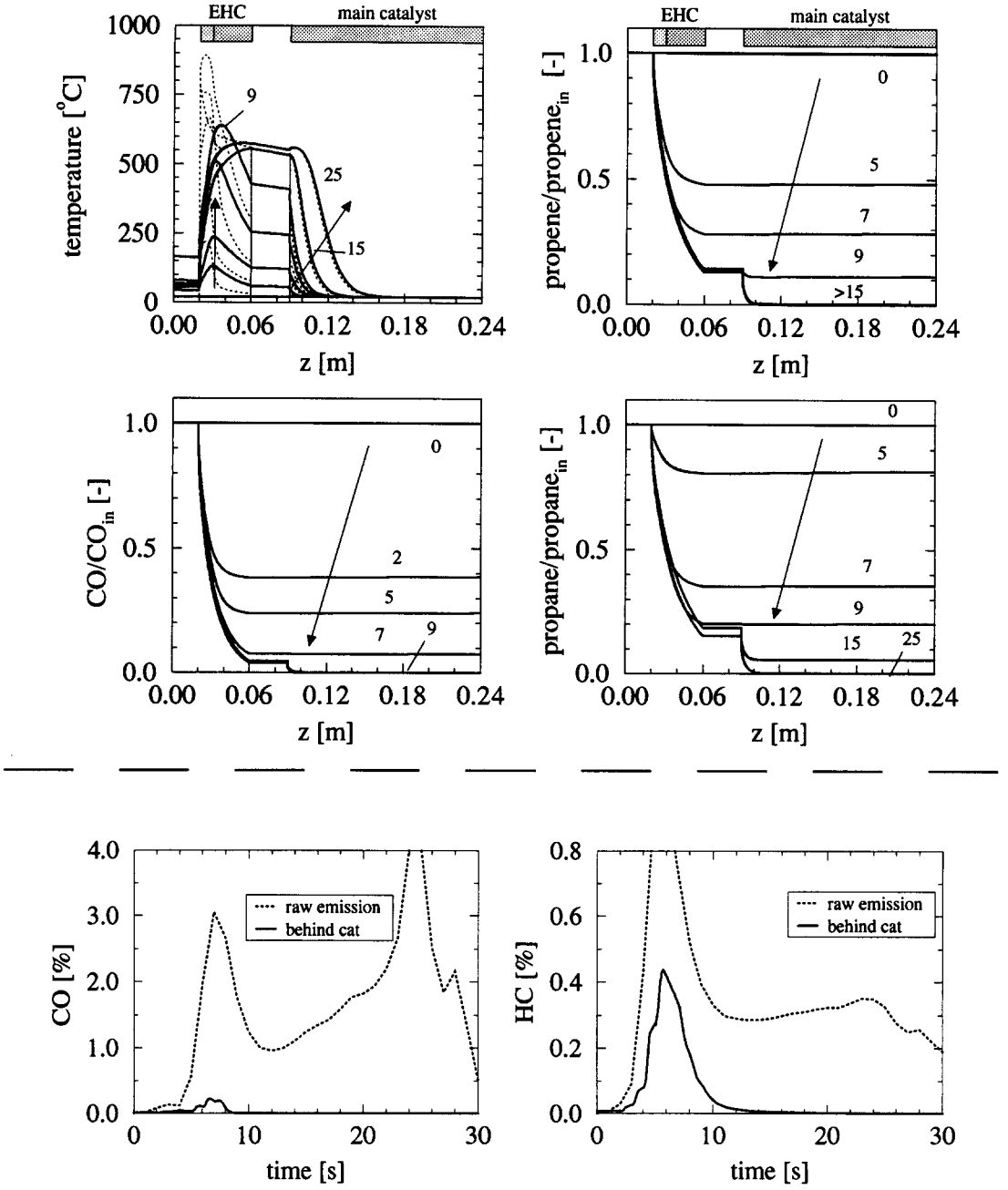

Fig. 5. Cold-start behavior using an electrically heated pre-catalyst (all times are given in seconds).

hot spot at $z \approx 0.09$ m (diagrams in the third column of Fig. 8). This temperature peak reaches a local temperature rise of approximately 400°C. It lasts only for a few second since the amount to CO on the catalyst is quickly consumed.

As mentioned before, the temperature of the exhaust gas stream is also rising while the car is accelerated. Now the entrance of the monolith is heated and the light-off temperature of the CO combustion is reached at the beginning of the catalyst.

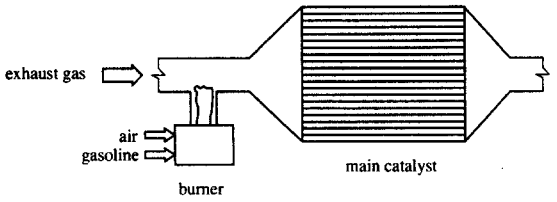

Fig. 6. Burner-heated catalyst (BHC).

Thus more and more reaction takes place at the entrance of the catalyst. This leads to an additional hot spot within the first 2 cm of the monolith (diagrams in the last column of Fig. 8). The temperature rise of approximately 600°C is higher compared to the first hot spot due to the higher CO concentrations at the entrance of the catalyst. Because of the high conversion of CO at the first 2 cm of the catalyst, the hot spot in the back of the catalyst cools down very fast. The second hot spot moves towards the entrance of the monolith due to thermal backward conduction of heat in the solid phase.

The occurrence and location of a hot spot is strongly influenced by the local heat and mass transfer between the gas phase and the solid phase as well as by the thermal conductivity of the catalyst support. Having a good heat transfer, the catalytic surface is cooled by the exhaust gas stream and hot spots are depressed. A high thermal conductivity of the catalyst support may also suppress the occurrence of hot spots, as local temperature gradients can be better compensated. In contrast, a higher thermal conductivity leads to a faster movement of the hot spot. In the simulation studies hot spots always seem to be connected with a rapid increase of the exhaust gas flow. Additionally, a suitable axial temperature profile with temperature levels close to the ignition temperatures of the exhaust gas components is necessary.

The maximum temperature level of a hot spot is of course influenced by the amount of burned pollutants but also by the increase of the mass flow of the exhaust gas (Fig. 9). As mentioned before, the mass flow during idle operation of the engine was assumed as approximately 7 g/s. In that case no temperature peaks can be obtained if the rise of the mass flow is less than 400%, i.e., below 28 g/s. Above that level and with increasing concentration of the pollutant the maximum temperature of the hot spot increases distinctly.

It should be mentioned that the transient hot spot behavior described may remain unnoticed in simulation studies if numerical methods without an automatic space and time step control are used. In our case simulations have been performed with the PDEXPACK-software, developed in a joint cooperation with the Konrad-Zuse-Zentrum, Berlin [12,13].

This simple example may give an idea of the complex dynamic behavior of the catalytic converter system. In chemical reaction engineering a somewhat similar behavior is already well known as "wrong way behavior" of fixed bed reactors [14–17].

5. Conclusions

In order to describe dynamic operation of automotive catalytic converter systems a simulation tool which is based upon a one-dimensional two-phase model was developed. The transient behavior during cold-start was studied for different designs of automotive catalytic converter concepts. It was shown that the behavior of automotive catalyst during transient operation becomes more and more important to improve the efficiency of catalytic converters during cold-start. Experimental studies on this topic are difficult to perform and very costly. For this reason simulation studies are a helpful tool.

Some simplifying assumptions were used for the simulation studies of local and transient temperature peaks. It was shown that under suitable catalyst conditions a mass flow and temperature increase may cause hot spots. The influence of some parameters on the occurrence and the location of hot spots were discussed but further investigations are necessary to get a better understanding for the dynamic behavior of automotive catalytic converters.

6. Notation

a_{ext} (m^2/m^3)	external surface to volume area ratio of monolith
a_v (m^2/m^3)	geometrical surface to volume area ratio of monolith
a_x (m^2_{Pt}/m^3)	catalytic surface to volume area ratio of monolith
c_p $(kJ/kg \cdot K)$	specific heat capacity

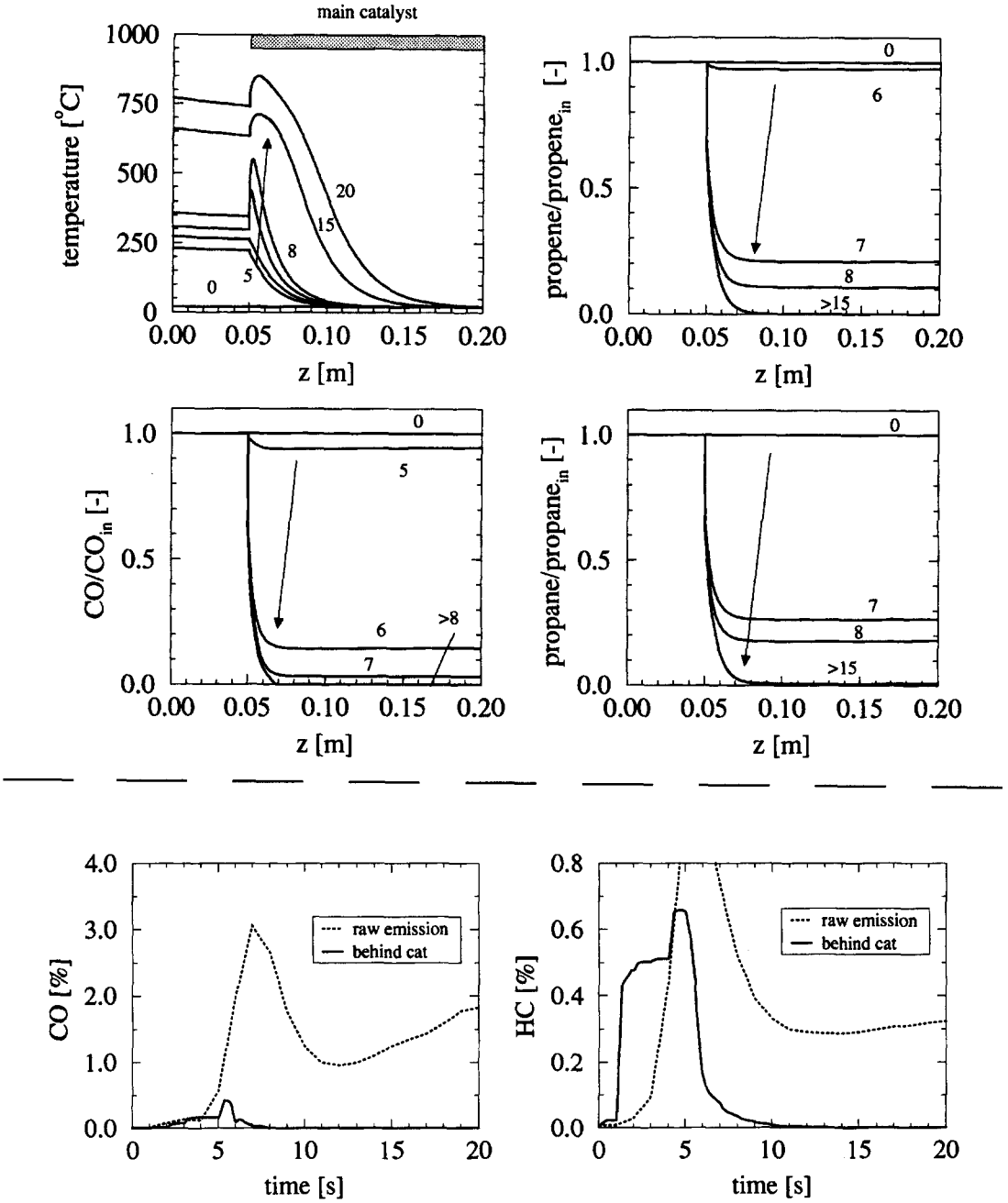

Fig. 7. Cold-start behavior using the BHC concept (all times are given in seconds).

D (kg/m · s)	dispersion coefficient	M_j (kg_j/$kmol_j$)	molar weight of component j
G_z (kg/m^2 · s)	specific mass flow	$\dot{q}$ (kW/m^2)	specific heat flux
Δh_R (kJ/kmol · s)	heat of reaction	R (kmol/m^2_{Pt} · s)	reaction rate
L (m)	length of monolith	t (s)	time

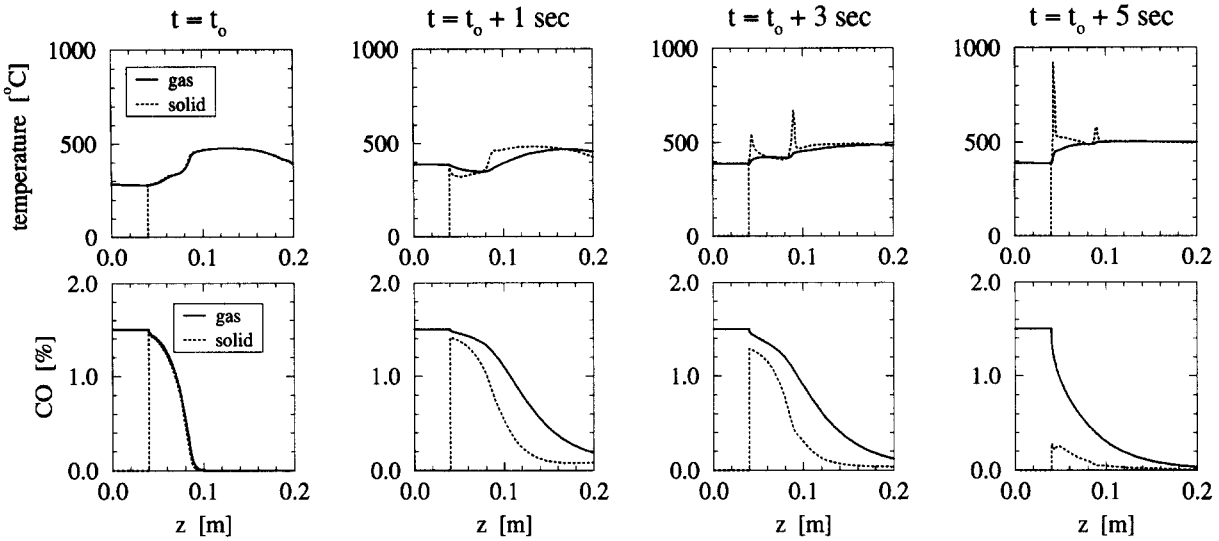

Fig. 8. Occurrence of hot spots during transient operation of automotive catalysts.

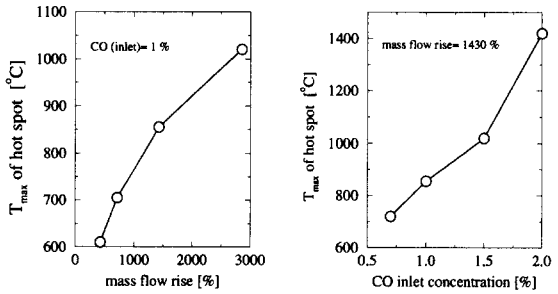

Fig. 9. Dependance of different parameters on the maximum hot spot temperature.

w_j (kg_j/kg)	weight fraction of component j
z (m)	spatial coordinate
α ($kW/m^2 \cdot K$)	heat transfer coefficient
β (m/s)	mass transfer coefficient
ϵ	void fraction
λ ($kW/m \cdot K$)	thermal conductivity
ν	stoichiometric coefficient
ρ (kg/m^3)	density
υ (°C)	temperature

Indices

amb	ambient
eff	effective
el	electrical
g	gas
i	reaction step i
in	inlet
j	component j
s	solid
z	spatial coordinate

Acknowledgements

Support of this work by Volkswagen AG is gratefully acknowledged.

References

[1] E. Koberstein and H. Völker, Chem. Ing. Tech., 50 (1978) 905–910.
[2] U. Hoffmann and A. Löwe, Chem. Ing. Tech., 58 (1986) 777–785.
[3] W.A. Whittenberger, J.E. Kubsh, SAE Technical Paper Series No. 900503 (1990).
[4] S. Roychodhury, D. Hixon, W. Pfefferle, R.E. Gibbs, W.J. Webster, R. Johnson, G. Wilson, SAE Technical Paper Series No. 940467 (1994).
[5] P. Pinkas, D. Snita, M. Kubicek and M. Marek, Chem. Eng. Sci., 49 (1994) 5347–5358.
[6] A. Donnerstag, A. Degen, M. Held, K. Korbel, VDI Fortschrittsberichte Reihe 12: Verkehrstechnik/Fahrzeugtechnik (239), 16 Internationales Wiener Motorensymposium, 1995..
[7] J.R. Mondt, ASME Trans. (1993) 461-467.

[8] P. Öser, E. Mueller, G.R. Härtel, A.O. Schürfeld, SAE Technical Paper Series No. 940474 (1994).
[9] K. Kollmann, J. Abthoff, W. Zahn, SAE Technical Paper Series No. 940469 (1994).
[10] T. Kirchner and G. Emgenberger, Chem. Eng. Sci., 51 (1996) 2409–2418.
[11] W. Held, A. Donnerstag, E. Otto, P. Küper, B. Pfalzgraf and A. Wirth, SAE Technical Paper Series No. 951072 (1995).
[12] U. Nowak, Adaptive Linienmethoden für nichtlineare parabolische Systeme in einer Raumdimension. TR 93–14, Konrad-Zuse-Zentrum für Informationstechnik Berlin, 1993.
[13] U. Nowak, J. Frauhammer and U. Nieken, Comp. Chem. Eng., 20 (1996) 547–561.
[14] H.S. Oh and J.C. Cavendish, Ind. Eng. Chem. Prod. Res. Dev., 21 (1982) 29–36.
[15] V. Pinjala, Y.C. Chen and D. Luss, AICHE J., 34 (1988) 1663–1672.
[16] Y.C. Chen and D. Luss, AICHE J., 35 (1989) 1148–1156.
[17] A. Il'in and D. Luss, AICHE J., 38 (1992) 1609–1617.